Positron emission tomography (PET) imaging of neuroblastoma and melanoma with ^{64}Cu-SarAr immunoconjugates

Stephan D. Voss*†, Suzanne V. Smith‡, Nadine DiBartolo‡, Lacey J. McIntosh§, Erika M. Cyr§, Ali A. Bonab§, Jason L. J. Dearling*, Edward A. Carter§, Alan J. Fischman§, S. Ted Treves*¶, Stephen D. Gillies‖, Alan M. Sargeson†**, James S. Huston‖, and Alan B. Packard*†¶

*Department of Radiology and ¶Division of Nuclear Medicine, Children's Hospital Boston, Harvard Medical School, 300 Longwood Avenue, Boston, MA 02115; ‡Australian National Science and Technology Organization (ANSTO), New Illawarra Road, PMB1, Menai, New South Wales 2234, Australia; §Division of Nuclear Medicine, Massachusetts General Hospital, Harvard Medical School, 55 Fruit Street, Boston, MA 02114; ‖Lexigen Research Center, EMD–Serono, 45A Middlesex Turnpike, Billerica, MA 01821-3936; and **Research School of Chemistry, Australian National University, Canberra ACT 0200, Australia

Contributed by Alan M. Sargeson, September 7, 2007 (sent for review May 11, 2007)

The advancement of positron emission tomography (PET) depends on the development of new radiotracers that will complement ^{18}F-FDG. Copper-64 (^{64}Cu) is a promising PET radionuclide, particularly for antibody-targeted imaging, but the high *in vivo* lability of conventional chelates has limited its clinical application. The objective of this work was to evaluate the novel chelating agent SarAr (1-*N*-(4-aminobenzyl)-3, 6,10,13,16,19-hexaazabicyclo[6.6.6]-eicosane-1,8-diamine) for use in developing a new class of tumor-specific ^{64}Cu radiopharmaceuticals for imaging neuroblastoma and melanoma. The anti-GD2 monoclonal antibody (mAb) 14.G2a, and its chimeric derivative, ch14.18, target disialogangliosides that are overexpressed on neuroblastoma and melanoma. Both mAbs were conjugated to SarAr using carbodiimide coupling. Radiolabeling with ^{64}Cu resulted in >95% of the ^{64}Cu being chelated by the immunoconjugate. Specific activities of at least 10 μCi/μg (1 Ci = 37 GBq) were routinely achieved, and no additional purification was required after ^{64}Cu labeling. Solid-phase radioimmunoassays and intact cell-binding assays confirmed retention of bioactivity. Biodistribution studies in athymic nude mice bearing s.c. neuroblastoma (IMR-6, NMB-7) and melanoma (M21) xenografts showed that 15–20% of the injected dose per gram accumulated in the tumor at 24 hours after injection, and only 5–10% of the injected dose accumulated in the liver, a lower value than typically seen with other chelators. Uptake by a GD2-negative tumor xenograft was significantly lower (<5% injected dose per gram). MicroPET imaging confirmed significant uptake of the tracer in GD-2-positive tumors, with minimal uptake in GD-2-negative tumors and nontarget tissues such as liver. The ^{64}Cu-SarAr-mAb system described here is potentially applicable to ^{64}Cu-PET imaging with a broad range of antibody or peptide-based imaging agents.

Positron emission tomography (PET) using the ^{18}F-labeled glucose analogue FDG (FDG-PET) has revolutionized the imaging of oncology patients by adding functional metabolic information to anatomic imaging data (1–3). This has become particularly important in the evaluation of newer therapeutic agents that inhibit tumor metabolism and proliferation without necessarily affecting tumor size (4). Although PET is now routinely used clinically, it may not reach its full potential in oncology unless significant advances are made with longer-lived PET isotopes, such as ^{64}Cu. Limitations to the chelating agents currently used with ^{64}Cu include significant loss of ^{64}Cu from the conjugate, leading to high uptake in the liver, and the requirement for postlabeling purification, typically by semipreparative HPLC. The further development of $^{64}Cu^{2+}$ imaging agents therefore requires Cu(II) chelators with (*i*) greater *in vivo* stability, (*ii*) improved labeling properties, and (*iii*) simplified conjugation to targeting molecules, such as antibodies, antibody fragments, and peptides (5).

Radiolabeled mAbs are established as agents in diagnosis and therapy, and interest in this field has increased of late, largely because of developments in antibody engineering. The *in vivo* stability and high specificity for target antigens make mAbs attractive vehicles for tumor-specific targeting of PET radionuclides. Imaging with radiolabeled mAbs directed against tumor-associated antigens has, however, been hampered in part by the limited number of radionuclides developed for use in radioimmunodiagnosis (5). Recently, antibody fragments and engineered antibody derivatives such as divalent synthetic single-chain Fv antibodies have been constructed in an effort to accelerate clearance kinetics, while maintaining tumor target specificity (6).

Copper-64 ($t_{1/2}$ = 12.7 h) decays by β^+ (20%) and β^- emission (37%), as well as electron capture (43%), making it well suited for radiolabeling antibodies, both for PET imaging (β^+) and therapy (β^+ and β^-) (5, 7–9). However, a major challenge to developing $^{64}Cu^{2+}$-based imaging agents has been identifying bifunctional chelating agents that stably complex $^{64}Cu^{2+}$ under physiological conditions (5, 10, 11). Such copper chelators must form complexes with high thermodynamic and kinetic stability and be resistant to *in vivo* processes such as transchelation to endogenous copper transport and binding proteins, and reduction to Cu^{1+}. Furthermore, the chemical conditions for conjugation and radiolabeling must be optimized to account for the biological and physical half-lives of the radioimmunoconjugate and to ensure that the specificity of the targeting agent is not impaired (5, 12).

A new class of bifunctional chelators has recently been synthesized (13) based on the hexaazamacrobicyclic sarcophagine cage Sar (Fig. 1) (14, 15). These compounds coordinate the Cu^{2+} ion within the multiple macrocyclic rings comprising the sarcophagine cage structure, yielding extraordinarily stable complexes that are inert to dissociation of the metal ion (5, 16). The Cu^{2+} cannot be removed from the cage under physiological conditions and thus resists transfer to copper-binding proteins

A preliminary account of this work was presented at the International Pediatric Radiology Fifth Conjoint Meeting, May 16–20, 2006, Montreal, Canada.

Author contributions: S.D.V., S.V.S., N.D., J.S.H., and A.B.P. designed research; S.D.V., L.J.M., E.M.C., A.A.B., and A.B.P. performed research; S.V.S., N.D., E.A.C., A.J.F., S.D.G., A.M.S., and J.S.H. contributed new reagents/analytic tools; S.D.V., S.V.S., J.L.J.D., S.T.T., J.S.H., and A.B.P. analyzed data; and S.D.V., S.V.S., J.S.H., and A.B.P. wrote the paper.

The authors declare no conflict of interest.

Abbreviation: PET, positron emission tomography.

†To whom correspondence may be addressed. E-mail: stephan.voss@childrens.harvard.edu, sargeson@rsc.anu.edu.au, or alan.packard@childrens.harvard.edu.

This article contains supporting information online at www.pnas.org/cgi/content/full/0708436104/DC1.

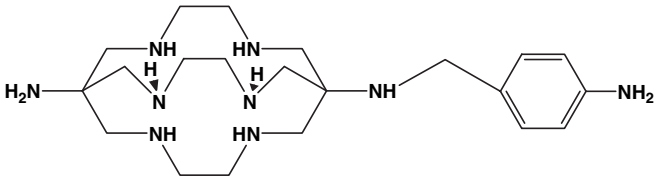

Fig. 1. Structure of SarAr. SarAr is based on the macrobicyclic cage diamsar and was modified to contain the reactive aminobenzyl group.

such as ceruloplasmin or superoxide dismutase. In fact, the Sar chelator can inhibit incorporation of copper into endogenous copper-binding proteins present in liver extracts (17). The Cu^{2+} ion within the Sar complex is also unusually resistant to reduction; in contrast, more facile *in vivo* reduction has compromised the utility of other copper radiopharmaceuticals (5, 18).

Smith *et al.* (13) have recently developed a derivative of the diamsar ligand, SarAr (Fig. 1), which incorporates an aromatic amine into the cage periphery. This allows SarAr to be readily cross-linked to carboxyl residues on peptides and antibody molecules via carbodiimide-mediated amide bonds. This cross-linking reaction can be carried out in neutral or slightly acidic pH conditions using standard aqueous buffers. The resulting SarAr immunoconjugates are stable, allowing for advance preparation and storage for future labeling with $^{64}Cu^{2+}$.

The data presented here extend earlier results characterizing the SarAr compound by demonstrating the feasibility of using this chelator to produce tumor-targeted immunoconjugates that can be readily labeled with $^{64}Cu^{2+}$ and used for *in vivo* imaging of neuroblastoma and melanoma. The procedures developed for this ^{64}Cu-SarAr-mAb system should also be applicable to the preparation of a broad range of ^{64}Cu-labeled protein-based PET imaging agents.

Results

Preparation and Characterization of SarAr-Conjugated ^{64}Cu-Labeled anti-GD2 Antibody Constructs. The SarAr ligand was successfully conjugated via its aromatic amine functional group to the ch14.18 antibody by using the 1-ethyl-3-(3-dimethylaminopropyl)-carbodiimide (EDC) reagent, forming a stable amide bond between the mAb and the chelator molecule. The optimal molar ratios of reagents were found to be a 500-fold excess of EDC to antibody, and a SarAr:IgG molar ratio of 250:1 in acetate buffer, pH 5.0 at 37°C for 30 min, consistent with earlier results (19).

Unbound SarAr was separated from the immunoconjugate by semipreparative HPLC, resulting in the purified immunoconjugate, SarAr-ch14.18. By using this procedure, up to 1.0 mg of immunoconjugate could be prepared in a single reaction, with no significant intramolecular IgG cross-linking detectable by HPLC or SDS/PAGE (data not shown), confirming earlier observations (19). Similar results were obtained with murine 14.G2a mAb and other immunoglobulins (data not shown), demonstrating the general applicability of this conjugation technique.

Radiolabeling of the SarAr-ch14.18 immunoconjugate was performed with carrier-free $^{64}Cu^{2+}$. The incorporation of copper into the immunoconjugate was complete within 10–30 min. By using a SarAr/IgG ratio of 250:1 and 10 μCi ^{64}Cu/μg of IgG, 95–99% labeling efficiency was routinely obtained (data not shown). The immunoreactivity of ^{64}Cu-labeled ch14.18 was confirmed by both RIA and direct cell binding studies. Under conditions of antigen excess, solid-phase RIA results showed that the SarAr-^{64}Cu labeling process did not adversely impact antibody immunoreactivity. There was 70% retention of control immunoreactivity (Fig. 2), consistent with results for other types of radioimmunoconjugates (20–22).

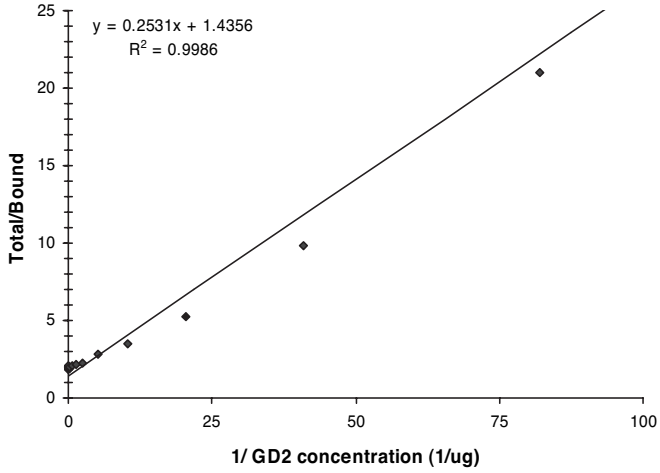

Fig. 2. Lindmo plot of GD2 binding data, confirming retention of immunoreactivity. Immunoreactive fraction of 70% was obtained [inverse *y* intercept (1/b = 1/1.4356)] by using a fixed concentration of labeled ch14.18 and increasing concentrations of GD2.

***In Vivo* Biodistribution of ^{64}Cu-Labeled ch14.18 mAb in Mice Bearing to GD2-Expressing Neuroblastoma and Melanoma Xenografts.** Fig. 3*A* shows representative biodistribution data from studies performed with M21 melanoma xenografts, which express high levels of GD2 on their cell surface [$\approx 15 \times 10^6$ sites per cell (23)]. Similar results, shown in Fig. 3*B*, were obtained with IMR-6 neuroblastoma xenografts, which express lower levels of GD2 [$\approx 10 \times 10^6$ sites per cell (24)]. These biodistribution studies

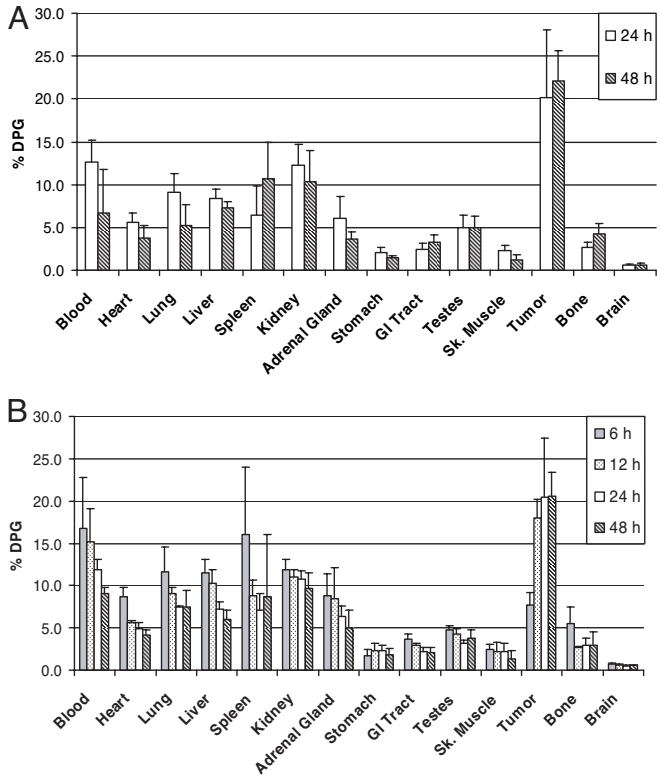

Fig. 3. *In vivo* biodistribution of [^{64}Cu]ch14.18 in neuroblastoma and melanoma xenograft-bearing animals. Data from athymic nude mice bearing s.c. M21 melanoma (*A*) or IMR6 neuroblastoma (*B*) human tumor xenografts are shown.

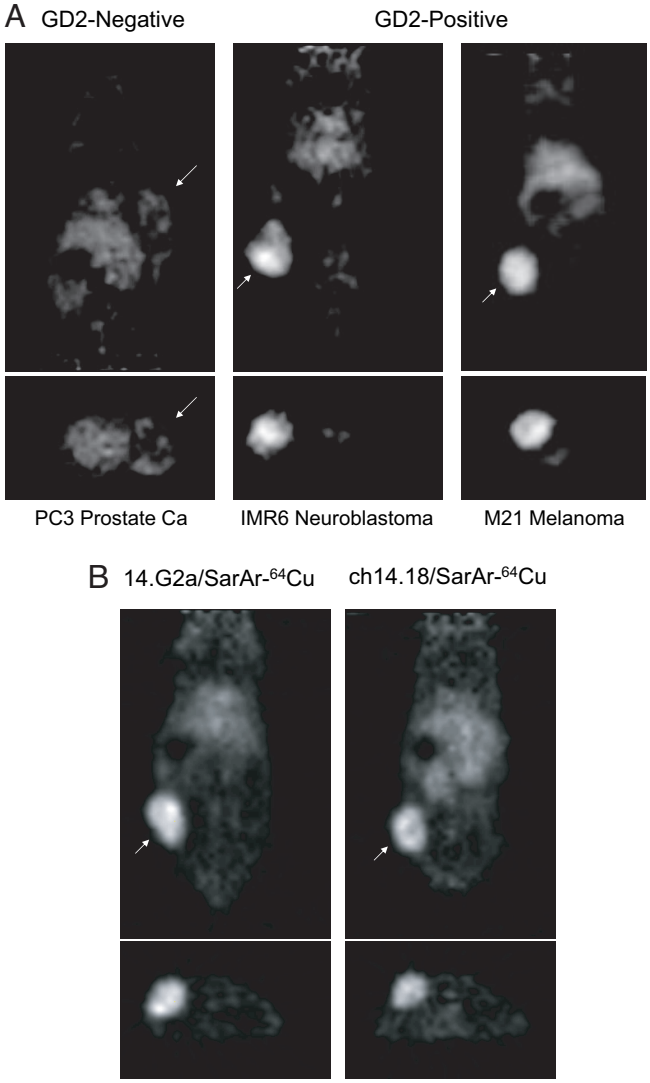

Fig. 4. MicroPET imaging of GD2-positive human tumor xenografts. Athymic nude mice bearing subcutaneous GD2-positive human tumor xenografts IMR6 neuroblastoma and M21 melanoma (*A*) and M21 melanoma (*B*) were injected with ^{64}Cu-labeled anti-GD2 mAb ch14.18 (*A* and *B*) or 14.G2a (*B*) and imaged. Control GD-2-negative PC-3 prostate carcinoma xenograft, treated and imaged similarly, is shown in *a*. Arrows point to flank tumors.

showed that 15–20% of the injected dose accumulated in the tumor at 24 h after injection (IMR-6 neuroblastoma 16.7 (±0.6%) ID/g; M21 melanoma 20.5 (±2.8%) ID/g). Note the retention of tracer in the tumor as clearance from the blood occurs over time.

MicroPET Imaging of GD2-Expressing Neuroblastoma and Melanoma Xenografts with ^{64}Cu-Labeled ch14.18 mAb. MicroPET imaging of selected animals bearing s.c. human tumor xenografts was performed at 24 h and 48 h after tracer injection (Fig. 4). High levels of ^{64}Cu-SarAr-ch14.18 were seen in GD2-positive tumors at 24 h (Fig. 4*A*), with only low levels of uptake in nontarget tissues. Tracer uptake in a GD2-negative PC3 prostate carcinoma xenograft, although slightly elevated over nontarget tissues, was less than that in the GD2-positive tumors and the liver (Fig. 4*A*). Similar results were seen with the parent murine mAb (14.G2a), from which the chimerized antibody ch14.18 was derived (Fig. 4*B*). The low level of liver uptake seen in these images is in agreement with the biodistribution data, emphasizing that SarAr, in contrast to other chelating agents, binds ^{64}Cu essentially irreversibly, with negligible loss to high-affinity endogenous copper-binding proteins. The complete 3-dimensional microPET image of the M21 melanoma xenograft is available in supporting information (SI) Movie 1.

Discussion

The data presented in this article demonstrate the feasibility of using the sarcophagine chelator SarAr to produce stable immunoconjugates that can be readily labeled with ^{64}Cu and used for *in vivo* tumor imaging. We have shown that SarAr conjugation to both murine and chimerized mAb can be accomplished under nearly physiological conditions with no adverse affect on immunoreactivity. Incubation of the immunoconjugate with $^{64}Cu^{2+}$ for 10–30 min results in nearly quantitative uptake of $^{64}Cu^{2+}$ without the need for additional HPLC purification, yielding specific activities of ≈10 μCi/μg (≈37 MBq/100 μg), 2–3 times greater than previously published results using other chelating agents (9, 25, 26). Furthermore, these high specific activities were achieved without the need for postlabeling purification, as is required with other chelators.

The bifunctional chelators most commonly used for labeling proteins with copper radionuclides are based on the tetraazamacrocyclic chelators DOTA and TETA (5). Copper is, however, lost from these ligands *in vivo* with concomitant accumulation in the liver (9, 27), where it is incorporated into endogenous copper-binding proteins, such as ceruloplasmin and superoxide dismutase (10, 28). Copper plays an important role in many normal physiological processes and, hence, is bound by a variety of circulating and intracellular proteins such as copper transporting ATPases, cytochrome oxidase, and superoxide dismutase. Copper is naturally excreted via liver hepatocytes; hepatic ceruloplasmin regulates recirculation and rerelease of copper into the plasma. Despite the high affinity of these endogenous proteins for copper, in our study, only 5–10% of the injected dose accumulated in the liver [8.3 (±1.0%) ID/g in neuroblastoma-bearing animals; 6.0 (±1.1%) ID/g in melanoma-bearing animals], which is consistent with normal hepatic clearance of an intact IgG. This is approximately one-half the value reported by others for liver uptake of ^{64}Cu-labeled DOTA immunoconjugates (9, 27).

A class of bicyclic tetraazamacrocycles, "cross-bridged" cyclam derivatives, has been developed that form highly stable complexes with Cu^{2+} and are less susceptible to *in vivo* transchelation than their nonbridged analogues (29). However, formation of these kinetically stable complexes requires more vigorous radiolabeling conditions (e.g., incubation at 75°C under basic conditions), which are likely to result in denaturation and hydrolysis of most antibodies and other complex macromolecules.

Earlier work with unconjugated SarAr showed that $[^{64}Cu(SarAr)]^{2+}$ complexes were stable in plasma, with no significant dissociation of the complex after 174 h (13). The $[^{64}Cu(SarAr)]^{2+}$ complex is rapidly excreted through the kidneys and, in contrast to other chelating agents, was not found to release copper into the liver (13). In the present study, we have extended these findings, showing tumor-specific uptake of SarAr-conjugated ^{64}Cu-labeled antineuroblastoma antibodies 14.G2a and ch14.18. Biodistribution studies showed rates of antibody clearance from the tissues that are expected for intact Ig molecules and are in agreement with earlier studies using iodinated derivatives of these same antibodies (23). At 24 h after injection, 15–20% of the injected dose accumulated in GD2-positive tumors, whereas only 5–10% of the injected dose accumulated in the liver. Low levels of liver uptake suggest that ^{64}Cu is not lost from SarAr, in contrast to results obtained with other chelating agents (9). Uptake by a GD2-negative xenograft was minimal (<5% ID/g). These results were confirmed by microPET imaging studies that showed high levels of ^{64}Cu-

SarAr-ch14.18 uptake in GD2-positive tumors, with low levels of background tissue uptake.

The longer half-life of ^{64}Cu (12.7 h) makes it attractive for radiolabeling antibodies, for both diagnosis and therapy. The focus of our study was to establish the feasibility of the use of ^{64}Cu-SarAr immunoconjugates for PET imaging of neuroblastoma and melanoma. The results shown here suggest that good tumor targeting of SarAr immunoconjugates is achieved in preclinical xenograft models of neuroblastoma and melanoma. Our current investigations are aimed at extending this work using engineered derivatives of the ch14.18 mAb to optimize pharmacokinetics and improve tumor-targeted PET imaging.

The aromatic amine incorporated into the periphery of the Sar cage allows SarAr to be readily cross-linked to carboxyl residues on antibodies via carbodiimide-mediated amide linkages, but other linkage strategies are also possible, the use of, for example, sulfhydryl or NHS ester-reactive SarAr derivatives. The effect of other linker strategies on the pharmacokinetics of the ^{64}Cu-SarAr-mAb system has yet to be investigated. The ability to quantitatively label these SarAr-modified compounds with radiolabeled copper in a single reaction thus allows for rapid screening and evaluation of multiple combinations of targeting molecules, chelators, and linker chemistries.

Finally, although we have not explored the use of SarAr for ^{67}Cu radioimmunotherapy, the extraordinarily high stability of the Cu-SarAr complex suggests that this chelator could be easily exploited to develop approaches for targeted radioimmunotherapy (30), both as a primary mode of treatment and in the adjuvant setting.

In conclusion, we have developed a tumor-specific PET imaging agent using neuroblastoma and melanoma as model systems. We have optimized the conjugation and radiolabeling procedure for ^{64}Cu PET imaging such that this procedure could be readily performed in any radiopharmacy by using routine techniques. The reactions can be performed under nearly physiologic conditions, and the ^{64}Cu-SarAr derivatives tested were shown to have high specific activity, antigen binding, and *in vivo* target specificity, with minimal uptake in normal tissues. The present investigation of ^{64}Cu-SarAr antibody targeting can easily be extended to other preclinical systems. These conjugates may also serve as the basis for development of a more specific PET imaging agent for neuroblastoma and melanoma.

Materials and Methods

Antibodies. The murine anti-GD2 antibody 14.G2a was purchased from Becton-Dickinson. The construction of the chimerized derivative of 14.G2a, ch14.18, has been described (31). The ch14.18 chimeric antibody shares only murine variable region sequences with 14.G2a; thus, these two antibodies have identical antigen-binding Fv regions, but contain distinct constant region sequences.

Cell Lines. The human melanoma cell line M21 has been described (23) and was generously provided by P. M. Sondel (University of Wisconsin, Madison, WI). NMB-7 and IMR-6 are both GD2-positive neuroblastoma cell lines that have been described (32), and were kindly provided by J. A. Denburg (McMaster University, Hamilton, ON, Canada). PC-3 human prostate adenocarcinoma cells were purchased from American Type Culture Collection (Manassas, VA). All cell lines were maintained in continuous culture in RPMI medium 1640 (M21, IMR-6, NMB-7) or Ham's F12 (PC-3) tissue culture medium supplemented with 10% FCS, penicillin/streptomycin, and L-glutamine.

SarAr Conjugation. Preparation of the SarAr chelator has been described in detail (13). The SarAr ligand was conjugated via its primary aromatic amino group to carboxyl groups on the 14.G2a and ch14.18 antibodies, in a reaction mediated by the carbodiimide reagent 1-ethyl-3-(3-dimethylaminopropyl)-carbodiimide (EDC). The use of the aromatic amine as a linker was shown to be essential (13) and allowed formation of a stable amide bond between glutamate or aspartate residues of monoclonal antibody and the chelator molecule. The optimal conditions for conjugation were a 500-fold molar excess of EDC to antibody, with a molar ratio of SarAr:IgG equal to 250:1 (19). The reaction was carried out in 0.1 M sodium acetate buffer, pH 5.0, at 37°C for 30 min.

Unbound SarAr was separated from the immunoconjugate by size-exclusion HPLC [BioSep SEC-S3000 column (Phenomenex, Torrance, CA)] with an isocratic aqueous phase consisting of 0.1 M sodium acetate, pH 5.0. Approximately 2 min separated elution of the immunoconjugate from unbound SarAr. The purified immunoconjugate fractions were pooled, concentrated by using a spin-column filter (Centricon; Millipore, Billerica, MA) (30,000 molecular mass cutoff), and stored in aliquots at −80°C. Based on serial dilution experiments with both $^{64}Cu^{2+}$ and $^{57}Co^{2+}$, an estimated four SarAr molecules are bound per antibody molecule, consistent with earlier results (19, 33), although the presence of trace amounts of contaminating metals in the $^{64}Cu^{2+}$ and $^{57}Co^{2+}$ isotope preparations could result in an underestimate of the actual total number of chelators present on the protein.

Radiolabeling with $^{64}Cu^{2+}$. The positron-emitting isotope $^{64}CuCl_2$ (radionuclide purity >99%) was provided by Michael J. Welch (Washington University, St. Louis, MO). Average specific activity at the time of shipping was 50 mCi/μg of Cu. The SarAr conjugated antibodies were incubated with 0.1 to 10 μCi of $^{64}Cu^{2+}$ per μg of antibody. The chelation reaction was performed in 0.1 M sodium acetate buffer, pH 5.0, for 30 min at 37°C. Similar results were obtained with shorter incubation times (10 min) and incubation at 21°C (data not shown). Labeling efficiency was determined by HPLC and TLC. By using 10 μCi of ^{64}Cu per μg of antibody, labeling efficiency was routinely 99%. For animal imaging experiments, 100–200 μg of antibody were typically labeled in a single procedure using 1–2 millicuries of $^{64}Cu^{2+}$.

Characterization of Immunoconjugates. Radioimmunoassays were performed by using disialoganglioside glycolipids immobilized on Immunolon microtiter plates. Purified gangliosides (Calbiochem, San Diego, CA) were resuspended in ethanol or DMSO. Microtiter wells were coated with saturating concentrations of purified disialoganglioside GD2 or GD1b (50 μg per well) and evaporated to dryness under a fume hood. Nonspecific sites were blocked with PBS, 1% BSA, and 0.01% Tween-20. Serial dilutions of the radiolabeled antibody were made into PBS/1% BSA and added to microtiter wells, followed by incubation at room temperature (i.e., 21°C) for 2 h. Plates were washed with PBS/1% BSA; the wells were then separated and counted in a γ-counter. In some experiments, a fixed concentration of radiolabeled ch14.18 antibody (the amount shown to produce 50% binding in conventional RIAs) was added to increasing concentrations of immobilized glycolipid; the binding data were then plotted by using the method of Lindmo (20), allowing an estimate of immunoreactive fraction after radiolabeling.

Animal Biodistribution Studies. All animal handling was done in accordance with Children's Hospital Boston and Massachusetts General Hospital Institutional Animal Care and Use Committee guidelines. Athymic (nu/nu) mice were used in this study and were purchased from The Jackson Laboratories (Bar Harbor, ME). Mice were injected s.c. with 2–5 × 10^6 M21, IMR-6 or PC-3 tumor cells by using Matrigel (1:1 vol:vol). By 5–7 weeks, tumors were growing exponentially and were typically 0.5–1 cm in diameter. For the biodistribution studies, animals were injected with 50–150 μCi (5–15 μg) of ^{64}Cu-labeled antibody via the

lateral tail vein. At selected time points after injection, animals were killed (four animals per time point), and major organs, blood samples, and tumors were weighed and assayed in a γ-counter. Several animals were imaged before killing for the biodistribution analysis. Results are presented as percent injected dose per gram of tissue (mean ± SD) (% ID/g).

MicroPET Imaging of GD2-Positive Tumor Xenografts. For the microPET imaging studies, mice were injected via the lateral tail vein with 50–150 μCi of ^{64}Cu-labeled antibody and imaged at 24 and 48 h after injection of the tracer by using a microPET P4 scanner (Concord Microsystems, Knoxville, TN). Just before imaging, mice were anesthetized (Ketamine 100 mg/kg, Xylazine 7 mg/kg, injected i.p.), placed in the prone position, and imaged in the scanner with the long axis of the mouse parallel to the long axis of the scanner. Acquisition time was typically 20 min by using a single bed position. Images were reconstructed by using filtered back projection with 2.2-mm resolution. After scanning, mice were killed, and tumors and other tissues were excised, weighed, and counted for biodistribution analysis.

We thank Pat Dunning for technical support, Nancy Drinan for editorial assistance, and John V. Frangioni, for guidance during the early stages of this investigation, which were supported by an American Association for Cancer Research–Amgen Research Fellowship in Clinical or Translational Research (to S.D.V.). We thank Dr. Michael Welch for providing ^{64}Cu, produced at Washington University School of Medicine (St. Louis, MO), under the support of National Cancer Institute Grant R24 CA86307.This work was supported by National Institutes of Health Grants 5K08CA093554 (to S.D.V.) and 5R01CA094338 (to A.B.P.) and the Ralf and Andrea Faber Fund for Radiological Research.

1. Rohren EM, Turkington TG, Coleman RE (2004) *Radiology* 231:305–332.
2. Gambhir SS (2002) *Nat Rev Cancer* 2:683–693.
3. Jerusalem G, Hustinx R, Beguin Y, Fillet G (2003) *Eur J Cancer* 39:1525–1534.
4. Wilkinson MD, Fulham MJ (2003) *Clin Nuclear Med* 28:780–781.
5. Smith SV (2004) *J Inorg Biochem* 98:1874–1901.
6. Wu AM, Senter PD (2005) *Nat Biotech* 23:1137–1146.
7. Anderson CJ, Connett JM, Schwarz SW, Rocque PA, Guo LW, Philpott GW, Zinn KR, Meares CF, Welch MJ (1992) *J Nucl Med* 33:1685–1691.
8. Connett JM, Buettner TL, Anderson CJ (1999) *Clin Cancer Res* 5:3207s–3212s.
9. Wu AM, Yazaki PJ, Tsai S, Nguyen K, Anderson AL, McCarthy DW, Welch MJ, Shively JE, Williams LE, Raubitschek AA, *et al.* (2000) *Proc Natl Acad Sci USA* 97:8495–8500.
10. Bass LA, Wang M, Welch MJ, Anderson CJ (2000) *Bioconjug Chem* 11:527–532.
11. Jones-Wilson TM, Deal KA, Anderson CJ, McCarthy DW, Kovacs Z, Motekaitis RJ, Sherry AD, Martell AE, Welch MJ (1998) *Nucl Med Biol* 25:523–530.
12. Sun X, Anderson CJ (2004) *Methods Enzymol* 386:237–261.
13. Di Bartolo NM, Sargeson AM, Donlev TM, Smith SV (2001) *J Chem Soc Dalton Trans*: 2303–2309.
14. Sargeson AM (1984) *Pure Appl Chem* 56:1603–1619.
15. Harrowfield JM, Herlt AJ, Lay PA, Sargeson AM (1983) *J Am Chem Soc* 105:5503–5505.
16. Sargeson AM (1996) *Coord Chem Rev* 151:89–114.
17. Bingham MJ, Sargeson AM, McArdle HJ (1997) *Am J Physiol* 272:G1400–G1407.
18. Barnhart-Bott A, Green MA (1991) *Int J Rad Appl Instrum B* 18:865–869.
19. Di Bartolo NM, Sargeson AM, Smith SV (2006) *Org Biomol Chem* 4:3350–3357.
20. Lindmo T, Boven E, Cuttitta F, Fedorko J, Bunn PA, Jr (1984) *J Immunol Methods* 72:77–89.
21. Ugur O, Kostakoglu L, Hui ET, Fisher DR, Garmestani K, Gansow OA, Cheung NK, Larson SM (1996) *Nucl Med Biol* 23:1–8.
22. Fonti R, Cheung NK, Bridger GJ, Guo HF, Abrams MJ, Larson SM (1999) *Nucl Med Biol* 26:681–686.
23. Mueller BM, Reisfeld RA, Gillies SD (1990) *Proc Natl Acad Sci USA* 87:5702–5705.
24. Cheung NK, Neely JE, Landmeier B, Nelson D, Miraldi F (1987) *J Nucl Med* 28:1577–1583.
25. Grunberg J, Novak-Hofer I, Honer M, Zimmermann K, Knogler K, Blauenstein P, Ametamey S, Maecke HR, Schubiger PA (2005) *Clin Cancer Res* 11:5112–5120.
26. Olafsen T, Kenanova VE, Sundaresan G, Anderson A-L, Crow D, Yazaki PJ, Li L, Press MF, Gambhir SS, Williams LE, *et al.* (2005) *Cancer Res* 65:5907–5916.
27. Cai W, Wu Y, Chen K, Cao Q, Tice DA, Chen X (2006) *Cancer Res* 66:9673–9681.
28. Mirick GR, O'Donnell RT, DeNardo SJ, Shen S, Meares CF, DeNardo GL (1999) *Nucl Med Biol* 26:841–845.
29. Boswell CA, Sun X, Niu W, Weisman GR, Wong EH, Rheingold AL, Anderson CJ (2004) *J Med Chem* 47:1465–1474.
30. DeNardo GL, Kennel SJ, Siegel JA, DeNardo SJ (2004) *Clin Lymphoma* 5:S5–S10.
31. Gillies SD, Lo KM, Wesolowski J (1989) *J Immunol Methods* 125:191–202.
32. Kushner BH, Cheung NK (1989) *Blood* 73:1936–1941.
33. Di Bartolo NM (2002) PhD thesis (Australian Natl Univ, Canberra, Australia).